

Cancer Prevention Research



Alcohol Consumption Promotes Diethylnitrosamine-Induced Hepatocarcinogenesis in Male Mice through Activation of the Wnt/ β -Catenin Signaling Pathway

Kelly E. Mercer, Leah Hennings, Neha Sharma, et al.

Cancer Prev Res 2014;7:675-685. Published OnlineFirst April 28, 2014.

Updated version Access the most recent version of this article at:
doi:[10.1158/1940-6207.CAPR-13-0444-T](https://doi.org/10.1158/1940-6207.CAPR-13-0444-T)

Supplementary Material Access the most recent supplemental material at:
<http://cancerpreventionresearch.aacrjournals.org/content/suppl/2014/04/28/1940-6207.CAPR-13-0444-T.DC1.html>

Cited Articles This article cites by 51 articles, 13 of which you can access for free at:
<http://cancerpreventionresearch.aacrjournals.org/content/7/7/675.full.html#ref-list-1>

E-mail alerts [Sign up to receive free email-alerts](#) related to this article or journal.

Reprints and Subscriptions To order reprints of this article or to subscribe to the journal, contact the AACR Publications Department at pubs@aacr.org.

Permissions To request permission to re-use all or part of this article, contact the AACR Publications Department at permissions@aacr.org.

Research Article

Alcohol Consumption Promotes Diethylnitrosamine-Induced Hepatocarcinogenesis in Male Mice through Activation of the Wnt/ β -Catenin Signaling PathwayKelly E. Mercer^{1,3}, Leah Hennings², Neha Sharma³, Keith Lai², Mario A. Cleves³, Rebecca A. Wynne³, Thomas M. Badger^{1,3}, and Martin J.J. Ronis^{1,3}**Abstract**

Although alcohol effects within the liver have been extensively studied, the complex mechanisms by which alcohol causes liver cancer are not well understood. It has been suggested that ethanol (EtOH) metabolism promotes tumor growth by increasing hepatocyte proliferation. In this study, we developed a mouse model of tumor promotion by chronic EtOH consumption in which EtOH feeding began 46 days after injection of the chemical carcinogen diethylnitrosamine (DEN) and continued for 16 weeks. With a final EtOH concentration of 28% of total calories, we observed a significant increase in the total number of preneoplastic foci and liver tumors per mouse in the EtOH+DEN group compared with corresponding pair-fed (PF)+DEN and chow+DEN control groups. We also observed a 4-fold increase in hepatocyte proliferation ($P < 0.05$) and increased cytoplasmic staining of active- β -catenin in nontumor liver sections from EtOH+DEN mice compared with PF+DEN controls. In a rat model of alcohol-induced liver disease, we found increased hepatocyte proliferation ($P < 0.05$); depletion of retinol and retinoic acid stores ($P < 0.05$); increased expression of cytosolic and nuclear expression of β -catenin ($P < 0.05$) and phosphorylated-glycogen synthase kinase 3 β (p-GSK3 β), $P < 0.05$; significant upregulation in Wnt7a mRNA expression; and increased expression of several β -catenin targets, including, glutamine synthetase (GS), cyclin D1, Wnt1 inducible signaling pathways protein (WISP1), and matrix metalloproteinase-7 (MMP7), $P < 0.05$. These data suggest that chronic EtOH consumption activates the Wnt/ β -catenin signaling pathways to increase hepatocyte proliferation, thus promoting tumorigenesis following an initiating insult to the liver. *Cancer Prev Res*; 7(7); 675–85. ©2014 AACR.

Introduction

Hepatocellular cancer (HCC) is one of the leading causes of cancer mortality in the world. In the United States, HCC incidence rates have significantly increased in past decades, which corresponds to the increased prevalence of risk factors in the population, including excessive alcohol consumption, chronic hepatitis C (HCV) or hepatitis B infections (HBV), and the metabolic syndrome (1–3). Interestingly, of these factors, alcohol consumption is the dominant independent factor associated with increased risk. In a case-control study involving U.S. patients with HCC, heavy

alcohol consumption (≥ 80 g daily) was the primary contributing factor for one third of the reported cases (2). The authors also reported increased risk (2-fold) in patients with HCV/HBV infections or diabetes mellitus combined with chronic alcohol consumption. In addition, the synergistic effect between HCV/HBV infection and chronic alcohol abuse has also been reported in other countries where hepatitis infections are more prevalent (4, 5).

In rodent models of alcoholic liver disease, ethanol (EtOH) is metabolized by alcohol dehydrogenase (ADH) to acetaldehyde, and then further reduced to acetate by aldehyde dehydrogenase (ALDH). Acetaldehyde is a potent carcinogen shown to generate DNA damage and strand breaks by interfering with both DNA synthesis and repair mechanisms (6). Alcohol also induces the expression of cytochrome P450 (CYP) CYP 2E1, which not only participates in alcohol metabolism, but also activates environmental procarcinogens, i.e., dietary nitrosamines, while simultaneously producing reactive oxygen species and lipid peroxidation products. These reactive products damage DNA through adduct formation, and strand breaks, all of which increases mutagenicity, and initiates hepatocarcinogenesis (6–8).

Authors' Affiliations: Departments of ¹Pediatrics and ²Pathology at the University of Arkansas for Medical Sciences; and ³Arkansas Children's Nutrition Center, Little Rock, Arkansas

Note: Supplementary data for this article are available at Cancer Prevention Research Online (<http://cancerprevres.aacrjournals.org>).

Corresponding Author: Kelly E. Mercer, University of Arkansas for Medical Sciences, Arkansas Children's Nutrition Center, 15 Children's Way, Little Rock, AR 72202. Phone 501-364-2784; Fax 501-264-2818; E-mail: kmercer@uams.edu

doi: 10.1158/1940-6207.CAPR-13-0444-T

©2014 American Association for Cancer Research.

Apart from the initiation mechanisms, alcohol consumption has proliferative and tumor-promoting effects (9–15). Several signaling pathways have been implicated in this process. One of which is decreased retinoic acid receptor (RAR) signaling resulting from vitamin A depletion in alcoholic livers (11). In EtOH-treated rats, down-regulation of RAR signaling resulted in hepatocyte proliferation associated with increased expression of Wnt signaling targets, cyclin D1 and cJun. Moreover, loss of RAR signaling in transgenic mice expressing a dominant-negative form of RAR in the liver also resulted in increased nuclear β -catenin/TCF4 complex formation and tumor incidence (16). Another pathway associated with alcohol exposure is transforming growth factor alpha (TGF α) activation of the epidermal growth factor receptor (EGFR) and p42/p44 mitogen kinase (MAPK) and PI3K/AKT pathways (17, 18). Interestingly, in mice overexpressing c-Myc and TGF α in the liver, phenobarbital exposure significantly enhanced proliferation and progression in a subset of tumors with increased nuclear accumulation of β -catenin (18, 19).

A significant proportion of patients with HCC, including those from alcoholics, have tumors defined by activated β -catenin (20, 21). In these tumors, aberrant activation occurs through mutations found either in the β -catenin gene, primarily in the phosphorylation site for glycogen synthase kinase 3 β (GSK3 β), or in Axin1/2, a scaffolding protein necessary for targeting β -catenin for degradation (22, 23). However, studies using transgenic mice expressing mutant forms of β -catenin have shown that activation through mutations is not sufficient to initiate tumorigenesis, and suggest instead that Wnt/ β -catenin signaling participates in tumor promotion (22). In light of the published data showing an association of β -catenin activity with signaling pathways involved in EtOH-mediated proliferation, we developed a mouse model of tumor promotion using diethylnitrosamine (DEN) as the initiation agent to test whether long-term EtOH ingestion increases tumor multiplicity through increased β -catenin signaling. To eliminate any possible initiating effects in response to EtOH feeding, primarily through increased CYP 2E1 expression and activity, liquid diets were started 7 weeks after DEN injection. A Lieber-DeCarli EtOH liquid diet was maintained until sacrifice (4 months). At the same time, we used liver tissue from a previously published rat model of long-term, chronic alcoholic liver disease to mechanistically validate the hypothesis that chronic EtOH ingestion alone increases hepatocyte proliferation through an upregulation of Wnt signaling, resulting in increased expression of known progression markers of HCC.

Materials and Methods

Animals and experimental design

All experimental procedures involving animals were approved by the Institutional Animal Care and Use Committee at the University of Arkansas for Medical Sciences. Mice were housed in an Association Assessment and Accred-

itation of Laboratory Animal Care–approved animal facility. Forty, time-impregnated C57Bl/6 mice (The Jackson Laboratory) were used to generate male pups ($n = 51$), which received a single intraperitoneal injection of 10 mg/kg DEN on postnatal day (PND)14. Mice were weaned to and maintained on rodent chow (Harlan Laboratories) until PND60 at which time DEN-injected mice were randomly assigned to three weight-matched diet groups: a chow diet ($n = 17$, chow+DEN), an EtOH-containing Lieber-DeCarli liquid diet ($n = 15$, EtOH+DEN), and a corresponding pair-fed (PF) diet ($n = 18$, PF+DEN). All groups had access to water *ad libitum*. EtOH was added to the Lieber-DeCarli liquid diet (35% of energy from fat, 18% from protein, and 47% from carbohydrates) by slowly substituting EtOH for carbohydrate calories (Dyets Inc.) in a stepwise manner until 28% of total calories was reached. This dose constitutes a final EtOH concentration of 4.9% (v/v), respectively, and was maintained until sacrifice (4 months). PF+DEN mice were fed the control diet (Dyets Inc.), which was isocalorically matched to the diet consumptions of the EtOH group. At sacrifice, mouse livers were perfused with 10% neutral buffered formalin (NBF, approximately 10 mL) *in situ*, removed, and stored in 10% NBF. Blood alcohol concentrations were analyzed using an Analox analyzer as previously reported (24). In a replicate study, 30 male mice were injected with DEN (10 mg/kg, PND14). At PND60, mice were randomized ($n = 10$) into chow+DEN, PF+DEN, and EtOH+DEN diet groups. Diets were maintained for 4 months as described above. At sacrifice, liver pieces were flash-frozen in liquid nitrogen and stored at -70°C . RNA isolated from these livers was transcribed to cDNA according to the manufacturer's instructions (iScript cDNA synthesis, Bio-Rad Laboratories) and used in real-time PCR analysis of tumor necrosis factor α (TNF α), interleukin 6 (IL6), CD14, and chemokine CXCL2. Results were quantified using ΔC_T method relative to 18s and then to chow+DEN controls. Primer sequences are presented in Supplementary Table S1.

Pathologic evaluation

In situ fixed mouse livers were stored in formalin for a minimum of 48 hours. Each liver lobe was sliced at 3-mm intervals, paraffin-embedded, sectioned (4 μm), stained, and examined in a blinded fashion under a light microscope by a veterinary pathologist (L. Hennings). Lesions were counted at $\times 40$ magnification. Preneoplastic foci were defined as follows: a basophilic focus, defined as a non-compressive lesion less than the width of four hepatic lobules in which hepatocytes are smaller and stain more basophilic than normal, and an eosinophilic focus, defined as a non-compressive lesion less than the width of four hepatic lobules in which hepatocytes are slightly larger than normal with more acidophilic cytoplasm. Preneoplastic foci can develop into adenomas, which were defined as a compressive lesion of any size without evidence of invasion or other criteria of malignancy, and may develop into HCC, which was defined as a compressive and invasive lesion with criteria of malignancy (25).

Immunohistochemistry

β -Catenin expression was assessed in liver sections by immunohistochemistry using standard procedures and a monoclonal β -catenin antibody (1:75) detecting the active, dephosphorylated (Ser37 or Thr41) form (anti-active β -catenin, clone 8E7; EMD Millipore). Quantification of β -catenin staining was achieved by color deconvolution using Aperio Technologies Spectrum analysis algorithm package and ImageScope analysis software. Proliferating cell nuclear antigen (PCNA) staining was assessed by immunohistochemistry following standard procedures and an anti-PCNA antibody (Abcam). Stained slides were evaluated under a light microscope. Nuclei of S-phase cells stained dark brown; a total of 10 observations ($\times 100$ field counted) were screened per liver sample. Data are expressed as mean \pm SE of total positive S-phase cells counted per sample in each group. Fibrosis was detected histologically by the Sirius Red/Fast Green Collagen Staining Kit (Chondrex) as per the manufacturer's instructions. Fibrosis staging was scored by a pathologist (K. Lai) blinded to the groupings using the Kleiner/Brunt scoring method: 0, no fibrosis; 1, sinusoidal, periportal, or portal only; 2, zone 3 and periportal; and 3, bridging fibrosis. α -SMA staining was performed using standard procedures and a monoclonal α -SMA antibody (1:100, Clone 1A4; Dako) and evaluated under a light microscope.

LC/MS-MS analysis of retinoid concentrations in EtOH-treated rat livers

All tissue processing, preparation, and extraction occurred in a fume hood, under a red light. Liver tissue (500 mg) was homogenized in 1 mL of Dulbecco's phosphate-buffered saline solution using a Precellys homogenizer (Bertin Technologies). Tissue homogenate was added to a glass screw-capped tube covered by aluminum foil. After adding the internal standard (250 μ L, 4,4-retinyl acetate) and 0.025 mol/L KOH to the homogenate, retinoids were extracted in hexane, and dried under a nitrogen stream. Retinoid extracts were reconstituted in 200 μ L of acetonitrile and separated by high-performance liquid chromatography (HPLC) using an Agilent 1100 HPLC system (Agilent Technologies) using Phenomenex Synergi 4 μ m Max-RP 80A column (4 μ m, 3 \times 150 mm) as previously described (11). Retinol and retinoic acid were identified using a 4000 QTRAP mass spectrometer (Applied Biosystems) coupled with the HPLC. The mass spectrometer was controlled using Analyst version 1.5.1 software and was operated in a multiple reaction monitoring (MRM) mode. Optimum positive atmospheric pressure chemical ionization (APCI) conditions included curtain gas, 30.0; collision gas, medium; nebulizer current, 3; temperature, 500°C; and GS1, 60. Peak area measurements were used to quantify retinoid amounts using standard curves based on retinol or retinoic acid and normalized using the internal standard.

Protein isolation and Western blotting

Frozen liver samples from a previously published study of chronic alcoholic liver disease were also analyzed (14).

Nuclear and cytosolic protein fractions were isolated from the total enteral nutrition (TEN) control and EtOH-treated rat livers using the NE-PER Nuclear and Cytoplasmic Extraction reagent Kit (Fisher Scientific). Blotted proteins were incubated with the anti-active β -catenin antibody, or with a polyclonal antibody recognizing the phosphorylated form of GSK3 β , [phospho-GSK3 α/β (Ser21/9); Cell Signaling Technology]. Expression of the pro and active forms of matrix metalloproteinase-7 (MMP7) was determined in blotted total lysate fractions using a polyclonal anti-MMP7 antibody (Sigma-Aldrich). Primary antibodies were diluted in at 1:1,000 and incubated overnight at 4°C. Secondary antibodies were diluted (1:10,000 to 1:50,000) and incubated at room temperature before chemiluminescence detection. Protein bands were quantified using a densitometer and band densities were corrected for total protein loaded by staining with 0.1% amido black.

Gene expression

RNA was isolated from livers acquired from a previously published rat model of alcoholic liver disease (14). Gene expression of cyclin D1, Ki67, glutamine synthetase (GS), and regucalcin was analyzed in duplicate ($n = 9$ per group). Results were quantified using the ΔC_T method relative to $B2M$ and expressed as mean \pm SEM. Samples from the TEN and TEN+EtOH groups were pooled ($n = 3$) separately, reversed transcribed using the iScript cDNA Synthesis Kit (Bio-Rad Laboratories), and analyzed for gene expression using a WNT signaling pathway RT² profiler PCR Array (#PARN 043Z; SABiosciences). Arrays for each group were performed in triplicate, and results were analyzed using a Web based analysis software provided by the manufacturer. Array data are presented in Supplementary Table S2. Genes with changes in fold expression greater than 1.5 and genes with fold changes that were significant, $P < 0.05$, were further analyzed by real time RT-PCR using individual cDNA samples from each group ($n = 9$), SYBR Green, and an ABI 7500 sequence detection system (Applied Biosystems). Results were quantified using the ΔC_T method relative to $\beta 2M$, and then to TEN controls. Gene-specific primers are presented in Supplementary Table S1.

Data and statistical analysis

Data presented as mean \pm SE. Comparisons between two groups were accomplished using either the student t test or Mann-Whitney U rank-sum test. Number of lesions was compared across groups using negative binomial regression, which generalizes Poisson regression to account for overdispersion of the count data. The proportion of new adenomas (incidence) was compared across groups using logistic regression. Both of these models included group membership as a set of indicator (dummy) variables. Continuous outcomes, such as PCNA and β -catenin were compared across groups using nonparametric Kruskal-Wallis rank test, and significant findings were followed by Bonferroni adjusted Wilcoxon/Mann-Whitney U rank-sum test for *post hoc* comparisons. Statistical analysis was performed using the SigmaPlot software package 11.0 (Systat Software,

Inc.) and Stata statistical software 13.1 (Stata Corporation). Statistical significance was set at $P < 0.05$.

Results

Study design and observations

In Fig. 1A, DEN-treated male mice were assigned to an EtOH liquid diet, a PF liquid diet, or standard chow 46 days after DEN injection. Starting weights for the mice were $23.9 \text{ g} \pm 0.35$, $23.2 \text{ g} \pm 0.26$, and $23.7 \text{ g} \pm 0.272$ for chow-fed, PF, and EtOH, respectively. EtOH feeding continued for 16 weeks. On average, the EtOH+DEN group received 21 g/kg/day of EtOH, which resulted in a mean (\pm SEM) blood alcohol concentration of $75 \pm 29 \text{ mg/dL}$ (range, 13–393) and is consistent with blood alcohol concentrations reported in persons legally intoxicated in the United States (26). At sacrifice, weight gain was lower in the chow+DEN and EtOH+DEN groups compared with the PF+DEN group, i.e., $29.0 \pm 0.3 \text{ g}$ and $32.4 \pm 0.5 \text{ g}$ versus $40.2 \pm 0.6 \text{ g}$, respectively ($P < 0.05$). Similar results were observed in the replicate study (data not shown). The difference in weight gain between EtOH and PF groups has been reported previously (24) and has been suggested to be a result of additional disruptive effects of EtOH on endocrine signaling and white adipose tissue differentiation (27, 28).

EtOH feeding increases tumor multiplicity but not incidence in DEN-treated mice

Liver lobes taken from chow+DEN, PF+DEN, and EtOH+DEN groups were assessed for presence of lesions, which encompassed basophilic and eosinophilic foci and adenomas (Fig. 1B). A small number of mice in the PF+DEN and EtOH+DEN groups had presented carcinomas, 0.22 (4 of 18) and 0.13 (2 of 15), respectively, but numbers were insufficient for statistical analysis. Basophilic foci were identified in all DEN-treated mice regardless of diet. Incidence of eosinophilic foci was increased in the DEN-treated mice receiving EtOH, 0.53 (8 of 15), compared with the PF+DEN, 0.17 (3 of 18), and chow+DEN, 0.12 (2 of 17), control groups, $P < 0.05$. Likewise, eosinophilic multiplicity was also greater in the EtOH+DEN group compared with DEN-treated PF and chow-fed groups, 0.86 ± 0.27 , 0.16 ± 0.09 , and 0.17 ± 0.12 , respectively, $P < 0.05$. Overall, we observed a significant increase in the total number of lesions present in the EtOH+DEN livers compared with the chow+DEN and PF+DEN groups (Fig. 1C). Adenoma incidence was greater in the PF+DEN and EtOH+DEN groups in comparison with the chow+DEN group ($P < 0.05$). However, we did not observe further increases in adenoma incidence following EtOH feeding, 0.60 versus 0.55, in the EtOH+DEN and PF+DEN group, respectively (Fig. 1D). Adenoma multiplicity was

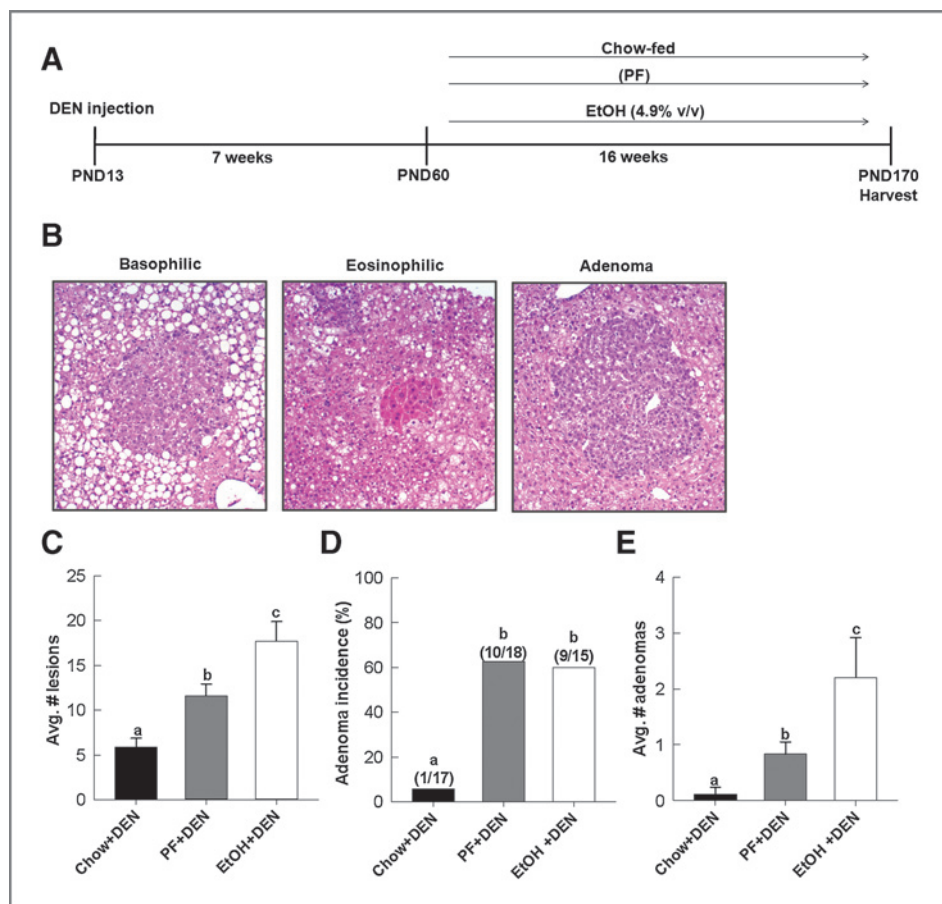


Figure 1. Chronic EtOH feeding enhances liver tumorigenesis in DEN-treated mice. A, experimental design; B, representative sections of hepatic lesions present in all groups; C, quantification of all lesions per group; D, adenoma incidence; and E, adenoma multiplicity per mouse for each group, chow+DEN ($n = 17$), PF+DEN ($n = 18$), and EtOH+DEN ($n = 15$). Data are expressed as mean \pm SE. Significance, a<b<c; $P < 0.05$.

significantly increased in PF+DEN mice compared with chow+DEN mice ($P < 0.05$) and in the EtOH+DEN mice compared with both chow+DEN and PF+DEN groups, $P < 0.05$ (Fig. 1E).

Proinflammatory markers are elevated in DEN-treated mice receiving PF and EtOH diets

Progression of alcoholic and nonalcoholic fatty liver diseases share several signaling pathways, including TNF α -mediated injury (29, 30). We measured hepatic expression of TNF α in the different DEN-treated diet groups. TNF α mRNA expression increased significantly in the PF and EtOH groups compared with chow (Fig. 2A). IL6 expression also increased in the EtOH group compared with both DEN-treated PF and chow-fed groups, $P < 0.05$ (Fig. 2B). Corresponding to these findings, we also observed significant increases in CD14 and CXCL2 expression, suggesting increased monocyte infiltration and activation in PF+DEN and EtOH+DEN-treated livers compared with the chow+DEN group (Fig. 2C and D).

Assessment of fibrosis in DEN-treated PF and EtOH mice

Parenchymal collagen deposition was assessed histologically by Sirius Red/Fast Green staining the DEN-treated groups. A representative section from each group, chow+DEN, PF+DEN, and EtOH+DEN is shown in Fig. 3A–C. In stained sections that were identified as having adenoma tumors, fibrosis staging was scored. Overall, fibrosis, when present in the PF+DEN (1 of 6) and the EtOH+DEN (1 of 6), was mild (average score, 1). In both the PF+DEN and EtOH+DEN groups, we observed α SMA staining in the smooth muscle cells lining hepatic blood vessels (data not shown). In Fig. 3D and E we did observe

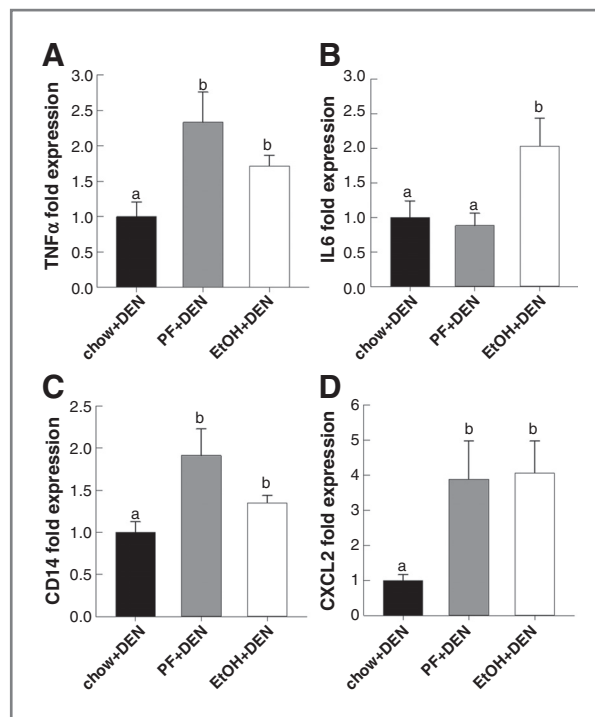
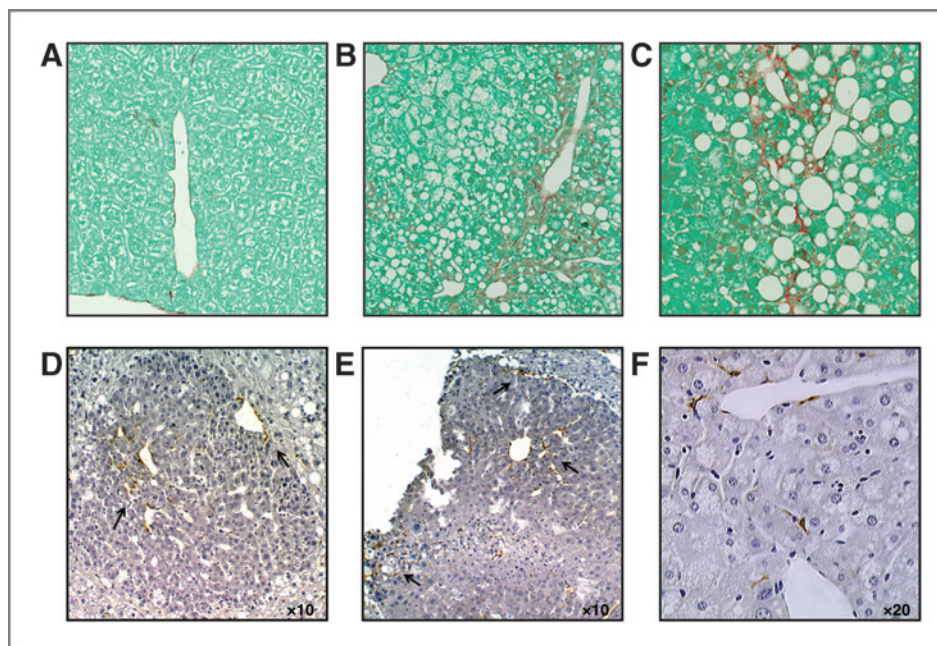


Figure 2. Relative mRNA expression of proinflammatory markers; A, TNF α ; B, IL6, and macrophage activation; C, CD14; D, CXCL2 in DEN-treated mice receiving different diets ($n = 10$ per group). Data are expressed as mean \pm SE. Significance, a<b<c; $P < 0.05$.

α SMA staining in and surrounding some of the larger adenomas (~ 0.90 mm \times 0.87 mm; W \times H) in the EtOH+DEN group. Adenomas of this size were not identified in the PF+DEN sections analyzed for α SMA. We also observed the presence of activated- α SMA-stained stellate

Figure 3. Sections representing the extent of fibrosis in A, chow+DEN; B, PF+DEN; and C, EtOH+DEN lobes identified to have adenomas ($\times 10$ magnification). Immunohistochemical staining of α SMA in D and E, adenomas from the EtOH+DEN group; and F, α SMA-stained stellate cells in nontumorigenic tissue of EtOH+DEN-treated mice ($\times 20$ magnification).



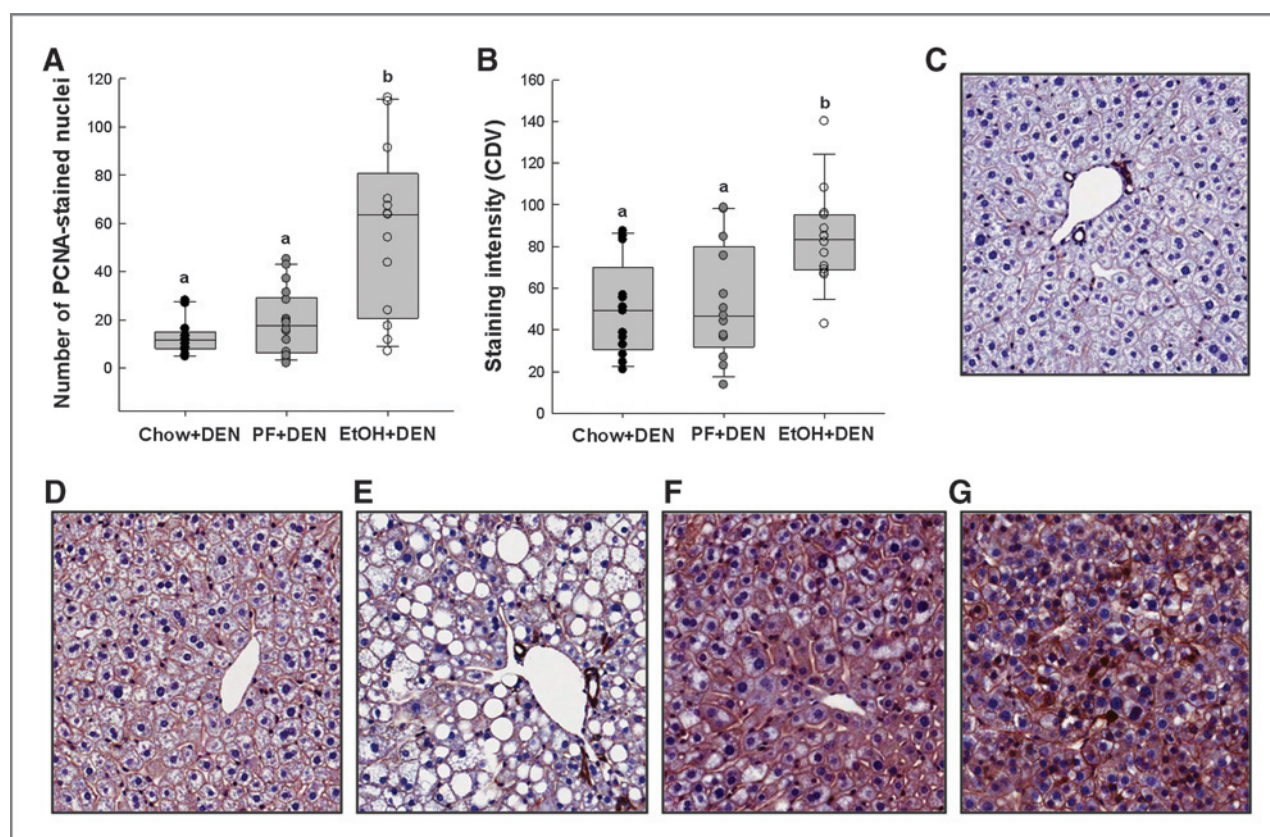


Figure 4. EtOH increases hepatocyte proliferation and β -catenin expression in nontumorigenic sections of chow+DEN ($n = 17$), PF+DEN ($n = 18$), and EtOH+DEN ($n = 15$) mice. A, staining intensity of PCNA; B, staining intensity of unphosphorylated (Ser41/33) β -catenin. Representative sections of C, chow control; D, chow+DEN; E, PF+DEN; and F, EtOH+DEN groups in comparison with G, β -catenin-stained adenoma arising in an EtOH+DEN-treated mouse ($\times 20$ magnification). Significance, $a < b < c$; $P < 0.05$.

cells in the parenchymal tissue in the EtOH+DEN-treated mice (Fig. 3F).

EtOH-mediated proliferation is associated with changes in β -catenin localization

In the EtOH+DEN-treated mice, tumor multiplicity corresponded to a 4-fold increase in the number of PCNA-stained nuclei present in the nontumorigenic tissue compared with DEN-treated chow and PF mice (Fig. 4A), suggesting hepatocyte proliferation, $P < 0.05$. Consistent with this finding, β -catenin staining in the EtOH+DEN-treated mice was significantly increased in comparison to both DEN chow and PF controls (Fig. 4B). Localization of β -catenin expression was also different between diet groups. In comparison with liver taken from an age-matched, chow-fed mouse (Fig. 4C), DEN treatment alone increased membrane expression of β -catenin in the Chow+DEN group (Fig. 4D). Similar to the chow+DEN group, β -catenin expression remains localized in the membrane of the PF+DEN-treated group (Fig. 4E). Unlike the other groups, in EtOH+DEN-treated mice we observed β -catenin staining in the membrane, cytosol, and in some areas nuclear β -catenin accumulation (Fig. 4F), which is a staining pattern similar to what we observed in tumor tissue (Fig. 4G).

EtOH feeding alone depletes hepatic retinoid stores in a TEN rodent model of ALD

Using a TEN rat model system of chronic alcohol consumption, we have previously shown that prolonged EtOH feeding (6 months) resulted in increased hepatocyte proliferation as measured by PCNA staining (14). In Table 1, further analysis of these samples by real time RT-PCR confirmed a 2-fold increase in Ki67 expression in the TEN+EtOH group compared with the TEN controls, $P < 0.05$. Chronic EtOH administration also significantly increased cyclin D1 expression, which is also a transcriptional target of β -catenin (31). Additional β -catenin targets, GS and regucalcin, were upregulated in the TEN+EtOH group compared with the TEN control, $P < 0.05$. This EtOH-associated proliferative phenotype was corresponded with depletion of hepatic retinoids, retinol, and retinoic acid; $P < 0.05$ in the TEN+EtOH compared with TEN control (Table 1).

EtOH feeding alone promotes Wnt/ β -catenin signaling in a TEN rodent model of ALD

β -Catenin expression and localization were assessed in cellular fractions prepared from TEN+EtOH and TEN control livers. In Fig. 5A, cytosolic expression of unphosphorylated β -catenin at serine residues 41 and 33 was increased in

Table 1. Hepatic markers of proliferation, β -catenin activity, and retinoid concentrations in a rat TEN model of alcoholic liver disease

Group	PCNA % S-phase	Gene expression (fold change)				Retinol nmol/g of liver	Retinoic acid nmol/g of liver
		Cyclin D1	Ki67	GS	Regucalcin		
TEN control	2.16 \pm 0.26 ^a	1.00 \pm 0.19 ^a	1.00 \pm 0.13 ^a	1.00 \pm 0.46 ^a	1.00 \pm 0.07 ^a	165.5 \pm 12.5 ^a	0.12 \pm 0.01 ^a
TEN+EtOH	3.64 \pm 0.68 ^b	2.29 \pm 0.59 ^b	2.45 \pm 0.46 ^b	4.47 \pm 1.58 ^b	1.48 \pm 0.12 ^b	113.1 \pm 8.8 ^b	0.08 \pm 0.01 ^b

NOTE: Data are expressed as mean \pm SE. PCNA staining presented has been published previously (14). Gene expression and determination of hepatic retinoid concentrations were carried out as described in Materials and Methods.

Statistical significance was determined by the Student *t* test. Significance, a<b; *P* < 0.05.

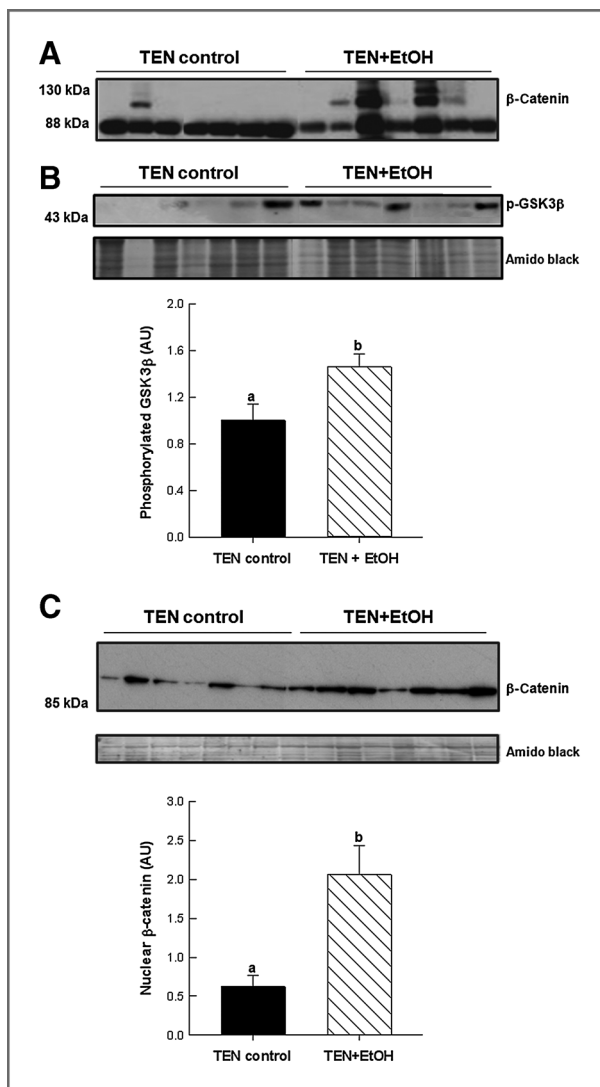


Figure 5. Western blot analysis of A, active, unphosphorylated (Ser41/33) β -catenin in the cytosol; B, phosphorylated GSK3 β in the cytosol; and C, nuclear accumulation of active β -catenin in EtOH-treated livers taken from the rat TEN model of chronic alcohol consumption. Data are expressed as mean \pm SE; densitometric values (*n* = 7 per group) were corrected for protein loading using amido black staining of whole lanes. Student *t* test. Significance, a<b; *P* < 0.05.

EtOH-treated livers compared with TEN controls, which also corresponded to an increase in the inactive, phosphorylated (Ser 21/9) GSK3 β in the TEN+EtOH group; *P* < 0.05 (Fig. 5B). In Fig. 5C, β -catenin expression was also significantly increased in the nucleus of in the TEN+EtOH group compared with TEN controls. In these EtOH-treated rats, increased accumulation of β -catenin in the nucleus corresponded to increased expression of genes involved in Wnt signaling pathways, as identified by an mRNA expression array and described in Materials and Methods. In Fig. 6A, EtOH increased expression of Wnt signaling mediators, Wnt2 and Wnt7a, by 2 to 3 fold; *P* < 0.05. There was also a corresponding increase in negative feedback mechanisms, including secreted frizzled related protein-1 (SFRP-1), and prickle-1 (*P* < 0.05), and a decrease in frizzled family receptor 5 (FZD), *P* = 0.072, in the EtOH+TEN group compared with TEN controls. Transcription factors associated with proliferation and cancer progression, cFos, transcription factor 3 (TCF3), and cMyc, were also unregulated in the TEN+EtOH group compared with TEN controls; *P* < 0.05 (Fig. 6B). Likewise, mRNA expression of Wnt1 inducible signaling pathways protein 1 (WISP1), and mRNA and protein expression of MMP7 were significantly increased in EtOH-treated livers compared with their corresponding control group (Fig. 6B and C).

Discussion

Although mechanisms underlying alcohol-induced initiation have been well characterized, alcohol-related signaling pathways involved in tumor promotion and progression are not as well delineated. In this study, we developed a mouse model of tumor promotion using DEN as the initiating agent, followed by chronic EtOH feeding. In response to EtOH treatment, we observed enhanced tumor progression in DEN-treated EtOH mice. Increased tumor multiplicity was associated with increased cytosolic and nuclear β -catenin expression and proliferation in hepatic nontumorigenic tissues. These results are consistent with the findings of Yip-Schneider and colleagues (15) who reported an increase in tumor multiplicity in male alcohol-preferring rats receiving EtOH in their drinking water compared with pair-matched rats on water alone. Brandon-Warner and colleagues have also reported increased tumor

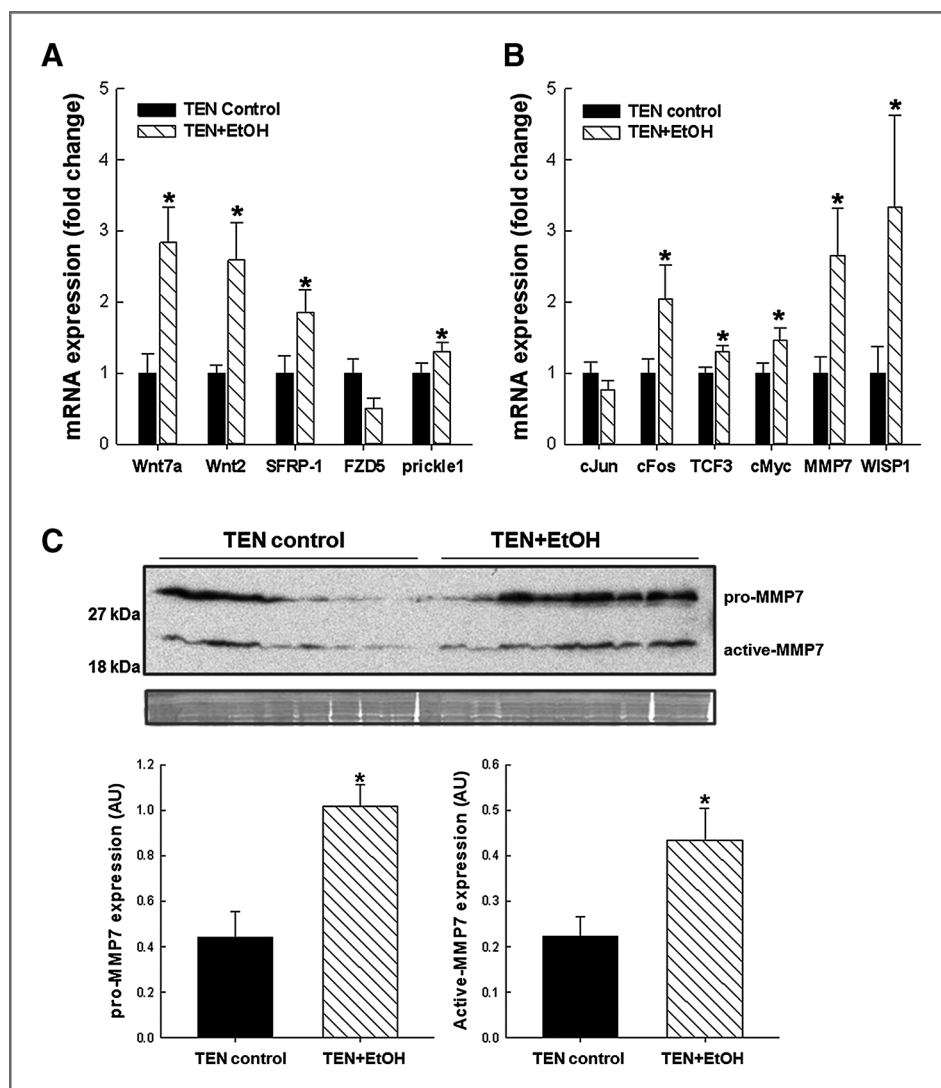


Figure 6. Relative mRNA expression of A, Wnt signaling mediators and components; and B, β -catenin targets in EtOH-treated rat livers compared with controls. Gene expression ($n = 9$ per group) was measured by real-time PCR and normalized to β -actin mRNA and then to TEN controls. C, upregulation of MMP7 mRNA corresponded to increased protein expression of pro-MMP7 (28 kDa) and active-MMP7 (19 kDa) in lysates from EtOH-treated livers. Data represent mean \pm SE; densitometric values ($n = 9$ per group) were corrected for protein loading using amido black staining of whole lanes. Student t test: *, $P < 0.05$ EtOH versus TEN control.

burden corresponding to a hepatic proliferative response in male DEN-treated mice receiving EtOH in the drinking water, suggestive of an EtOH-related promotional effect (10). However, we did not observe a significant increase in tumor incidence in the EtOH+DEN group compared with the PF+DEN group. In this study, increased tumor incidence was specifically associated with high fat (35%) feeding, which corresponded to an increase in $\text{TNF}\alpha$ signaling and macrophage recruitment. Recently, Wang and colleagues have demonstrated that an extremely high fat diet (70%) also produces nonalcoholic steatohepatitis (NASH), which promoted hepatic carcinogenesis in DEN-treated rats associated with increased $\text{TNF}\alpha$ signaling, and increased hepatocyte proliferation (32). In our model, the PF diet (35% fat) alone does not stimulate proliferation, or alter β -catenin cellular localization as observed in the DEN-treated EtOH group. Taken together, these findings and those reported by Wang and colleagues suggest that dietary effects on hepatocyte proliferation and tumorigenesis may be dose-dependent on fat intake, mediated by

$\text{TNF}\alpha$ signaling, but do not involve direct activation of β -catenin.

In a separate rodent model alcoholic liver disease (the rat TEN model), EtOH feeding inactivates GSK3 β activity through phosphorylation, which disrupts sequential phosphorylation of β -catenin necessary for proteasomal degradation, thus increasing β -catenin translocation to the nucleus. As a result, Wnt/ β -catenin targets were upregulated, including soluble Wnt mediators and suppressors, indicative of an inhibitory feedback loop in response to chronic activation of canonical Wnt signaling. Previously, we have shown in rats that low-dose EtOH exposure (urine ethanol concentration, UEC < 500 mg/dL) improves hepatic insulin sensitivity, resulting in increased phosphorylation of GSK3 β through insulin substrate receptor (IRS1)/AKT signaling (33). Therefore, the possibility exists that insulin signaling may also be contributing to the overall increase in β -catenin activity. Another potentially important finding that is clinically relevant in alcoholic patients is the subsequent depletion of hepatic retinoic acid stores in rats

following chronic EtOH feeding. Basic research has shown that EtOH metabolizing enzymes, ADH and ALDH, participate in retinoid metabolism, and in the liver, EtOH inhibits retinol conversion to retinoic acid through substrate competition (34). In addition, EtOH-mediated induction of CYP 2E1 further increases enzymatic degradation of retinoic acid to polar metabolites (35, 36). In mice, loss of retinoid signaling corresponds with increased β -catenin activation, proliferation, and tumorigenesis in the liver (37). A potential mechanism may be the suppression of retinoid acid receptor (RAR) inhibitory effect on Wnt/ β -catenin signaling through direct binding and removal of β -catenin from transcriptional machinery (38). In animals, low-dose supplementation of retinoic acid during EtOH exposure restores hepatic retinoid concentrations, ameliorates alcoholic liver injury, and reverses EtOH-mediated hepatocyte proliferation in rats (11,37). Our findings, in light of these reports, suggest a link between increased β -catenin activity and proliferation to EtOH-mediated retinoid depletion.

There are other pathways that may also be involved in increasing β -catenin activity following chronic alcohol exposure. Hepatocyte growth factor (HGF) is a potent mitogen for liver regeneration after injury, which binds to its tyrosine kinase receptor, Met, to stimulate proliferation (39). In animal models of liver regeneration using partial hepatectomy, alcohol exposure inhibits HGF-mediated proliferation and repair (40). However, in patients with acute alcoholic hepatitis, hepatic HGF expression correlates with proliferation and patient survival (41). Likewise, there is one report showing increased hepatic HGF expression in male rats receiving liquid EtOH diets (42). Interestingly, Monga and colleagues have identified a membrane-bound Met/ β -catenin complex by which β -catenin nuclear translocation and subsequent expression of target genes occurs through tyrosine phosphorylation resulting from HGF/Met activation (43). In addition to tyrosine kinase signaling, there is also some evidence to support a role for noncanonical Wnt signaling through cJun NH2 terminal kinase (JNK) activation in modulating β -catenin translocation and activation (44, 45). Many of the Wnt targets we identified as upregulated following EtOH exposure are also transcriptionally regulated by JNK through cJun. Wnt7a, a proposed mediator for noncanonical Wnt/JNK signaling (46), is also highly expressed in our EtOH-treated rat hepatocytes. Moreover, in some cancer types, Wnt7a increases cJun phosphorylation and subsequent proliferation of cancer cells (47, 48). At this time, it is unknown whether tyrosine kinase receptor and/or JNK signaling are involved in EtOH-mediated β -catenin activation in our carcinogenesis model, and this issue warrants further investigation.

In conclusion, we have developed a new DEN-induced hepatocarcinogenesis mouse model designed to identify EtOH-specific mechanisms involved in tumor promotion

and progression. In response to EtOH feeding, DEN-treated mice have increased tumor burden, which corresponded to increased hepatocyte proliferation and increased β -catenin expression and nuclear localization in non tumor hepatic tissue. In a separate study, EtOH feeding alone reduced hepatic retinoid concentrations, increased hepatocyte proliferation and nuclear expression of β -catenin, and increased expression of established markers of HCC progression. Generally speaking, aberrant β -catenin activity in HCC has been associated with gene mutation (22, 23). Likewise, tumorigenesis associated with DEN-treated mice receiving phenobarbital is also dependent on mutant-specific β -catenin activation (49, 50). However, in these DEN/phenobarbital mice, mutations within β -catenin occur late (>32 weeks), following the development of chromosomal instability (49). In our mouse model, we observed β -catenin activation and translocation at 16 weeks, which puts forward the possibility that chronic increases in Wnt/ β -catenin signaling apart from acquired mutations may also participate in sensitizing the liver to tumor initiating and promoting insults. Currently, there are no clinical strategies for lowering HCC risk in alcoholics, particularly in recovering alcoholics, whose HCC risk does not decrease with abstinence (7). In the literature, there are several plant-derived phytochemicals with anticancer properties, some of which are known to inhibit β -catenin signaling pathways (51). We believe that future studies using this animal model will provide valuable information on the molecular mechanisms whereby EtOH acts as a tumor promoter, and insight into potential dietary interventions that may be beneficial in lowering HCC risk in alcoholic populations.

Disclosure of Potential Conflicts of Interest

No potential conflicts of interest were disclosed.

Authors' Contributions

Conception and design: K.E. Mercer, M.J.J. Ronis

Development of methodology: K.E. Mercer

Acquisition of data (provided animals, acquired and managed patients, provided facilities, etc.): K.E. Mercer, R.A. Wynne

Analysis and interpretation of data (e.g., statistical analysis, biostatistics, computational analysis): L. Hennings, N. Sharma, K. Lai, M.A. Cleves, M.J.J. Ronis

Writing, review, and/or revision of the manuscript: K.E. Mercer, L. Hennings, N. Sharma, K. Lai, M.A. Cleves, M.J.J. Ronis, T.M. Badger

Administrative, technical, or material support (i.e., reporting or organizing data, constructing databases): L. Hennings, N. Sharma, K. Lai, R.A. Wynne, M.A. Cleves, T.M. Badger

Grant Support

This work was funded by grants from the NIH (AA0118282 and CA169389).

The costs of publication of this article were defrayed in part by the payment of page charges. This article must therefore be hereby marked *advertisement* in accordance with 18 U.S.C. Section 1734 solely to indicate this fact.

Received January 7, 2014; revised April 2, 2014; accepted April 20, 2014; published OnlineFirst April 28, 2014.

References

- Altekruse SF, McGlynn KA, Reichman ME. Hepatocellular carcinoma incidence, mortality, and survival trends in the United States from 1975 to 2005. *J Clin Oncol* 2009;27:1485-91.
- Hassan MM, Hwang LY, Hatten CJ, Swaim M, Li D, Abbruzzese JL, et al. Risk factors for hepatocellular carcinoma: synergism of alcohol with viral hepatitis and diabetes mellitus. *Hepatology* 2002;36:1206-13.

3. Welzel TM, Graubard BI, Zeuzem S, El Serag HB, Davila JA, McGlynn KA. Metabolic syndrome increases the risk of primary liver cancer in the United States: a study in the SEER-Medicare database. *Hepatology* 2011;54:463–71.
4. Chen CJ, Liang KY, Chang AS, Chang YC, Lu SN, Liaw YF, et al. Effects of hepatitis B virus, alcohol drinking, cigarette smoking and familial tendency on hepatocellular carcinoma. *Hepatology* 1991;13:398–406.
5. Mohamed AE, Kew MC, Groeneveld HT. Alcohol consumption as a risk factor for hepatocellular carcinoma in urban southern African Blacks. *Int J Cancer* 1992;51:537–41.
6. Poschl G, Seitz HK. Alcohol and cancer. *Alcohol Alcohol* 2004;39:155–65.
7. Morgan TR, Mandayam S, Jamal MM. Alcohol and hepatocellular carcinoma. *Gastroenterology* 2004;127:S87–96.
8. Seitz HK, Stickel F. Molecular mechanisms of alcohol-mediated carcinogenesis. *Nat Rev Cancer* 2007;7:599–12.
9. Baumgardner JN, Shankar K, Korourian S, Badger TM, Ronis MJ. Undernutrition enhances alcohol-induced hepatocyte proliferation in the liver of rats fed via total enteral nutrition. *Am J Physiol Gastrointest Liver Physiol* 2007;293:G355–64.
10. Brandon-Warner E, Walling TL, Schrum LW, McKillop IH. Chronic ethanol feeding accelerates hepatocellular carcinoma progression in a sex-dependent manner in a mouse model of hepatocarcinogenesis. *Alcohol Clin Exp Res* 2012;36:641–53.
11. Chung J, Liu C, Smith DE, Seitz HK, Russell RM, Wang XD. Restoration of retinoic acid concentration suppresses ethanol-enhanced c-Jun expression and hepatocyte proliferation in rat liver. *Carcinogenesis* 2001;22:1213–19.
12. Isayama F, Froh M, Yin M, Conzelmann LO, Milton RJ, McKim SE, et al. TNF alpha-induced Ras activation due to ethanol promotes hepatocyte proliferation independently of liver injury in the mouse. *Hepatology* 2004;39:721–31.
13. Ronis MJ, Butura A, Korourian S, Shankar K, Simpson P, Badeaux J, et al. Cytokine and chemokine expression associated with steatohepatitis and hepatocyte proliferation in rats fed ethanol via total enteral nutrition. *Exp Biol Med* 2008;233:344–55.
14. Ronis MJ, Hennings L, Stewart B, Bashnagian AG, Apostolov EO, Albano E, et al. Effects of long-term ethanol administration in a rat total enteral nutrition model of alcoholic liver disease. *Am J Physiol Gastrointest Liver Physiol* 2011;300:G109–19.
15. Yip-Schneider MT, Doyle CJ, McKillop IH, Wentz SC, Brandon-Warner E, Matos JM, et al. Alcohol induces liver neoplasia in a novel alcohol-preferring rat model. *Alcohol Clin Exp Res* 2011;35:2216–25.
16. Yanagitani A, Yamada S, Yasui S, Shimomura T, Murai R, Murawaki Y, et al. Retinoic acid receptor alpha dominant negative form causes steatohepatitis and liver tumors in transgenic mice. *Hepatology* 2004;40:366–75.
17. Hennig M, Yip-Schneider MT, Klein P, Wentz S, Matos JM, Doyle C, et al. Ethanol-TGFalpha-MEK signaling promotes growth of human hepatocellular carcinoma. *J Surg Res* 2009;154:187–95.
18. Thoresen GH, Guren TK, Sandnes D, Peak M, Agius L, Christoffersen T. Response to transforming growth factor alpha (TGFalpha) and epidermal growth factor (EGF) in hepatocytes: lower EGF receptor affinity of TGFalpha is associated with more sustained activation of p42/p44 mitogen-activated protein kinase and greater efficacy in stimulation of DNA synthesis. *J Cell Physiol* 1998;175:10–18.
19. Calvisi DF, Ladu S, Factor VM, Thorgeirsson SS. Activation of beta-catenin provides proliferative and invasive advantages in c-myc/TGF-alpha hepatocarcinogenesis promoted by phenobarbital. *Carcinogenesis* 2004;25:901–8.
20. Edamoto Y, Hara A, Biernat W, Terracciano L, Cathomas G, Riehle HM, et al. Alterations of RB1, p53 and Wnt pathways in hepatocellular carcinomas associated with hepatitis C, hepatitis B and alcoholic liver cirrhosis. *Int J Cancer* 2003;106:334–41.
21. Zucman-Rossi J, Jeannot E, Nhieu JT, Scoazec JY, Guettier C, Rebouissou S, et al. Genotype-phenotype correlation in hepatocellular adenoma: new classification and relationship with HCC. *Hepatology* 2006;43:515–24.
22. Nejak-Bowen KN, Monga SP. Beta-catenin signaling, liver regeneration and hepatocellular cancer: sorting the good from the bad. *Semin Cancer Biol* 2011;21:44–58.
23. Villanueva A, Newell P, Chiang DY, Friedman SL, Llovet JM. Genomics and signaling pathways in hepatocellular carcinoma. *Semin Liver Dis* 2007;27:55–76.
24. Mercer KE, Wynne RA, Lazarenko OP, Lumpkin CK, Hogue WR, Suva LJ, et al. Vitamin D supplementation protects against bone loss associated with chronic alcohol administration in female mice. *J Pharmacol Exp Ther* 2012;343:401–12.
25. Cardiff RD, Anver MR, Boivin GP, Bosenberg MW, Maronpot RR, Molinolo AA, et al. Precancer in mice: animal models used to understand, prevent, and treat human precancers. *Toxicol Pathol* 2006;34:699–707.
26. Dillner L, Josefson D, Karcher H, Sheldon T, Dorozynski A, Zinn C. Alcohol—pushing the limits. *BMJ* 1996;312:7–9.
27. Crabb DW, Zeng Y, Liangpunsakul S, Jones R, Considine R. Ethanol impairs differentiation of human adipocyte stromal cells in culture. *Alcohol Clin Exp Res* 2011;35:1584–92.
28. Ronis MJ, Wands JR, Badger TM, de la Monte SM, Lang CH, Calisendorff J. Alcohol-induced disruption of endocrine signaling. *Alcohol Clin Exp Res* 2007;31:1269–85.
29. Abdelmegeed MA, Banerjee A, Yoo SH, Jang S, Gonzalez FJ, Song BJ. Critical role of cytochrome P450 2E1 (CYP2E1) in the development of high fat-induced non-alcoholic steatohepatitis. *J Hepatol* 2012;57:860–66.
30. Farrell GC, Larter CZ. Nonalcoholic fatty liver disease: from steatosis to cirrhosis. *Hepatology* 2006;43:S99–12.
31. Tan X, Behari J, Cieply B, Michalopoulos GK, Monga SP. Conditional deletion of beta-catenin reveals its role in liver growth and regeneration. *Gastroenterology* 2006;131:1561–72.
32. Wang Y, Ausman LM, Greenberg AS, Russell RM, Wang XD. Non-alcoholic steatohepatitis induced by a high-fat diet promotes diethylnitrosamine-initiated early hepatocarcinogenesis in rats. *Int J Cancer* 2009;124:540–46.
33. He L, Marecki JC, Serrero G, Simmen FA, Ronis MJ, Badger TM. Dose-dependent effects of alcohol on insulin signaling: partial explanation for biphasic alcohol impact on human health. *Mol Endocrinol* 2007;21:2541–50.
34. Wang XD. Chronic alcohol intake interferes with retinoid metabolism and signaling. *Nutr Rev* 1999;57:51–59.
35. Liu C, Russell RM, Seitz HK, Wang XD. Ethanol enhances retinoic acid metabolism into polar metabolites in rat liver via induction of cytochrome P4502E1. *Gastroenterology* 2001;120:179–89.
36. Liu C, Chung J, Seitz HK, Russell RM, Wang XD. Chlormethiazole treatment prevents reduced hepatic vitamin A levels in ethanol-fed rats. *Alcohol Clin Exp Res* 2002;26:1703–709.
37. Pan Z, Dan Z, Fu Y, Tang W, Lin J. Low-dose ATRA supplementation abolishes PRM formation in rat liver and ameliorates ethanol-induced liver injury. *J Huazhong Univ Sci Technolog Med Sci* 2006;26:508–12.
38. Easwaran V, Pishvaian M, Salimuddin, Byers S. Cross-regulation of beta-catenin-LEF/TCF and retinoid signaling pathways. *Curr Biol* 1999;9:1415–18.
39. Zarnegar R. Regulation of HGF and HGFR gene expression. *EXS* 1995;74:33–49.
40. Saso K, Higashi K, Nomura T, Hoshino M, Ito M, Moehren G, et al. Inhibitory effect of ethanol on hepatocyte growth factor-induced DNA synthesis and Ca²⁺ mobilization in rat hepatocytes. *Alcohol Clin Exp Res* 1996;20:330A–34A.
41. Fang JW, Bird GL, Nakamura T, Davis GL, Lau JY. Hepatocyte proliferation as an indicator of outcome in acute alcoholic hepatitis. *Lancet* 1994;343:820–23.
42. Tahara M, Matsumoto K, Nukiwa T, Nakamura T. Hepatocyte growth factor leads to recovery from alcohol-induced fatty liver in rats. *J Clin Invest* 1999;103:313–20.
43. Monga SP, Mars WM, Padiaditakis P, Bell A, Mule K, Bowen WC, et al. Hepatocyte growth factor induces Wnt-independent nuclear translocation of beta-catenin after Met-beta-catenin dissociation in hepatocytes. *Cancer Res* 2002;62:2064–71.

44. Saadeddin A, Babaei-Jadidi R, Spencer-Dene B, Nateri AS. The links between transcription, beta-catenin/JNK signaling, and carcinogenesis. *Mol Cancer Res* 2009;7:1189–196.
45. Wu X, Tu X, Joeng KS, Hilton MJ, Williams DA, Long F. Rac1 activation controls nuclear localization of beta-catenin during canonical Wnt signaling. *Cell* 2008;133:340–53.
46. Itoh T, Kamiya Y, Okabe M, Tanaka M, Miyajima A. Inducible expression of Wnt genes during adult hepatic stem/progenitor cell response. *FEBS Lett* 2009;583:777–81.
47. Carmon KS, Loose DS. Secreted frizzled-related protein 4 regulates two Wnt7a signaling pathways and inhibits proliferation in endometrial cancer cells. *Mol Cancer Res* 2008;6:1017–28.
48. Heasley LE, Winn RA. Analysis of Wnt7a-stimulated JNK activity and cJun phosphorylation in non-small cell lung cancer cells. *Methods Mol Biol* 2008;468:187–96.
49. Aleksic K, Lackner C, Geigl JB, Schwarz M, Auer M, Ulz P, et al. Evolution of genomic instability in diethylnitrosamine-induced hepatocarcinogenesis in mice. *Hepatology* 2011;53:895–904.
50. Stahl S, Ittrich C, Marx-Stoelting P, Kohle C, Altug-Teber O, Riess O, et al. Genotype-phenotype relationships in hepatocellular tumors from mice and man. *Hepatology* 2005;42:353–61.
51. Thakur R, Mishra DP. Pharmacological modulation of beta-catenin and its applications in cancer therapy. *J Cell Mol Med* 2013;17:449–56.